Sixth International Conference on the Durability of Concrete Structures **Paper Number PSE24**
18 - 20 July 2018
University of Leeds, Leeds, West Yorkshire, LS2 9JT, United Kingdom

Mechanical and Microstructure Characteristics of Concrete-Mixtures Designed for Durability of RC-Structures in Corrosive Environments

S.A. Alghamdi, S. Ahmad and M.M. Khaled
King Fahd University of Petroleum and Minerals, Dhahran 31261, KSA

ABSTRACT

As exposures to chloride-salts are known as prime factors causing initiation and continuity of corrosion-process of steel reinforcement bars in reinforced concrete (RC) structures, it has always been a major concern for designers considering the requirements of structural-durability for targeted-service life of RC-structures in aggressively corrosive environments typically prevalent in coastal regions. Research works previously reported by the researchers have modeled corrosion-process in terms of corrosion-current density, and it was realized that concrete-mixtures design quality and characteristics, degree of exposures to corrosive-agents such as chloride salts, and protective-concrete cover-thickness are now known beyond doubt to be determinant factors as regards RC-structures durability. This research paper is focused on presenting highlights of an extensive experimental investigation carried out on a large number of concrete specimens that were designed, and placed in chloride-salt solution simulating exposure to corrosion-conditions. Results presented in this paper include close-looks at mechanical and micro-structure characteristics with regard to the influence of key design-parameters and exposure-conditions used for test-specimens with various combinations of cementitious materials constituents and proportioning using three replicate-combinations of water-cementitious ratios, fine to total aggregate ratio, and concrete-cover thickness, and with different concentrations of chloride-solution. Statistical analysis of results obtained from a three-year test-program is outlined in terms of one unifying corrosion-process progress indicator, namely, corrosion-current density I_{corr}, determined by both electrochemical method and gravimetric weight-loss method. The paper presents a general overview of the test program and a summary of sample results on mechanical, strength, and microstructural characteristics obtained from test specimens.

Keywords: RC durability; reinforcement corrosion; corrosion current density

1.0 INTRODUCTION

Due to various combinations of environmental conditions (including excessive exposures to chloride salts) and sub-standard construction practices, corrosion of reinforcing steel has been known worldwide to be the main cause of deterioration of reinforced concrete (RC) structures and some premature structural failures even before designed-for service-life could be attained [Dyer, 2014; Gehlen and Schiessl, 1999; Ferreira 2010]. Numerous research efforts have been particularly designed to identify influential factors contributing to reinforcement corrosion and mechanisms of corrosion, with particular emphasis on the role of chloride ions [Page 1996; Bentur, *et al.* 1997; Oh, *et al.* 2004; Ali 2003; Mehta 1977]. Presence of *chloride ions* in concrete mixtures has also been identified to play a prominent role in initiation and progress of reinforcements corrosion of RC structures [Page 1996]. It is noted that as resulting corrosion-products have larger volume and induce stresses and strains that exceed tensile strength of concrete matrix, cracking and spalling of concrete cover result in loss of interlocking-bond between steel and concrete. Reduction in rebar diameter and loss of bond due to reinforcement corrosion cause a significant loss of load-bearing capacity of RC members [Morinaga 1990; Park, *et al.* 2008; Page, *et al.* 1986]. Assessments of influence of concrete construction materials and concrete-mixture design parameters and protective-cover thickness on service life of RC structures have been addressed in several previous research works [Mehta 1977; Ali 2003; Park, *et al.* 2008; Alghamdi and Ahmad 2010]. It is noted that while some experimental data have utilized electrochemical monitoring techniques to predict reinforcement corrosion over a reasonable period of time, the accuracy of reinforcement corrosion rates measured electrochemically [Al-Tayyib and Khan 1988; Power-CORR 2001] have been noted to be invariably doubtful because of difficulties and errors that are frequently prevalent in such experimental methods. Therefore, as these experimental techniques do lack accuracy and reliability in producing dependable design database for durability-based design purposes, an extensive experimental investigation was undertaken [Alghamdi and Ahmad 2010] using a large number of concrete test-specimens designed with various combinations of design variables including water-cementitious material ratio (*w/c*), cementitious material content,

fine to total aggregate ratio and protective-cover thickness for a monitoring period exceeding three years, and the results (that is electrochemically-measured corrosion rates) were compared to gravimetrically determined (weight-loss basis) corrosion rates. The comparative experimental program is complemented by analysis of strength, mechanical, and variance of test-results compiled for all test specimens. Moreover, the study included analysis of microstructure characteristics of sample specimens using scanning electron microscopy (SEM; Stutzman 2000) to closely inspect prevailing structural morphology of concrete matrix of typical test-specimens.

This paper aims at providing: i) a general overview of the experimental program used for corrosion-monitoring and assessment using concrete test specimens particularly prepared and grouped in four design-groups' combinations; ii) results depicting key features of strength, mechanical, and microstructural characteristics of test-specimens; and iii) recommendations to utilize the results for service-life prediction and/or design optimization for structural-durability of RC structures.

2.0 EXPERIMENTAL PROGRAM

2.1 Properties of construction materials

Type I Normal Portland Cement (Table 1-a) was used with *silica fume* added to all concrete-mixtures. Concrete specimens used in this study were made with aggregates obtained from two distant quarries in Dammam (H) and Taif (T) localities of east and west regions in Saudi Arabia. Specific gravity and water absorption were determined using ASTM standards [ASTM C128-07a, 2003] and abrasion test results of coarse aggregates in accordance with ASTM standards [ASTM C33-03, 2004] are summarized in Table 1-b. Specific gravity and absorption of fine aggregate were found to be 2.6% and 0.57%, *respectively*. And to enhance workability of concrete mixtures, superplasticizer was used for cases with low water-cement ratio.

2.2 Test specimens (mixtures designs and mechanical properties)

Steel bars of diameter 16 mm (i.e. steel reinforcement) were centrally placed in 486 cylindrical concrete specimens having one common height of 150 mm, three diameters of 66, 91, and 116 mm, and three values of cover thickness (C_V) of 25, 37.5, and 50 mm. Epoxy coating was applied to steel bar at bottom and at interface between concrete and air. Details of typical specimen is schematically shown in Fig. 1 (a).

Concrete mixture design proportions were determined using the absolute volume method with each constituent-quantity calculated weight-wise and 8% (by weight) silica fume is added to each mix. The water-cementitious ratio (w/c), cementitious material content (C_C) and fine to total aggregate ratio (FA/TA), were, w/c: 0.4, 0.45, and 0.5; C_C: 350, 375, and 400 kg/m^3; and FA/TA: 0.35, 0.4, and 0.45. The sodium chloride concentrations used were 3%, 7%, and 12%. A homogenous concrete was obtained with all constituents mixed together with addition of potable water and with a superplasticizer mixed uniformly with the constituents to enhance workability. Concrete mixtures with uniform consistency and cohesiveness (with no segregation of constituents) were obtained in one-minute using drum-type mixer.

Specimens were demolded after 24 hours of casting and were cured for a period of 28 days in water tanks under laboratory conditions. The specimens were then partly submerged in chloride solutions to allow corrosion to take place. Typical test specimens exposed to chloride solution are shown in Fig. 1(b), and Tables 2 and 3 provide a compiled summary of strength and mechanical properties for all of the 486 test specimens prepared for the test-program using the H-type and T-type specimens.

Table 1. Materials Characteristics and properties for aggregates and cementitious ingredients

a) Chemical composition of cement (Type I) and silica fume

Constituents (*wt* %)	Type I cement	Silica fume
Silica (SiO_2)	19.92	98.7
Alumina (Al_2O_3)	6.54	0.21
Ferric oxide (Fe_2O_3)	2.09	0.046
Lime (CaO)	64.70	0.024
Magnesia (MgO)	1.84	-
Silicate (SO_3)	2.61	0.015
Potassium Oxide (K_2O)	0.56	0.048
Sodium Oxide(Na_2O)	0.28	0.085
Tri-calcium Silicate (C_3S)	55.9	-
Di-calcium silicate (C_2S)	19	-
Tri-calcium aluminate (C_3A)	7.5	-
Tetra-calcium alumino-ferrite (C_4AF)	9.8	-

b) Specific gravity, absorption and abrasion test results of coarse aggregates

Aggregate source	Specific gravity	Water absorption (%)	Abrasion loss (%)
Dammam (H)	2.55	1.75	28.86
Taif (T)	2.82	1.27	37.84

2.3 Experimental procedures used (LPR vs. GMWL)

Linear polarization resistance method (LPRM)

Corrosion current density I_{corr} was determined using linear polarization resistance method (LPRM) using PARSTAT 2273 potentiostat [Power-CORR 2001]. Experimental set-up used for LPR measurement is schematically shown in Fig. 2. Measurement of I_{corr} was determined using a three-electrode system

composed of: i) reference electrode, ii) counter electrode (steel plate) connected to respective terminals of the potentiostat, and iii) steel reinforcement in concrete specimen (known as *working electrode*) was polarized to ±20 mV from its equilibrium potential at a scan rate of 0.166 mV/second.

Then after suitable initial delay of about 60 seconds, the steel bar was polarized to determine the polarization curve. A typical curve is shown in Fig. 3, and the slope of applied potential *versus* measured current plot is used to determine linear polarization resistance, R_p. Corrosion current density I_{corr} is then calculated using the following relationship:

$$I_{corr} = \frac{B}{R_p} \quad (1)$$

where:

I_{corr} = corrosion current density (μA/cm^2)
R_p = polarization resistance (kΩ . cm^2)

$$B = \frac{\beta_a \beta_c}{(\beta_a + \beta_c)} \quad (2)$$

with anodic and cathodic Tafel constants β_a and β_c. Tafel constants are generally obtained from Tafel plot [Al-Tayyib and Khan 1988], and in absence of such plot, *B*-values of 52 mV, and 26 mV may be used for steel-bars in *passive* and active states, *respectively*. In this study, the *B*-value used was 26 mV.

Gravimetric weight loss method (GWLM)

Upon completion of all rounds of corrosion monitoring using LPR method, all test-specimens were broken-up in order to determine corrosion rates by gravimetric weight loss method. Experimental set-up and typical specimens collected and prepared for this purpose are shown in Fig. 4. Preparation, cleaning and estimation of weight-loss were done according to ASTM standards [ASTM G1-03, 2003]. Cleaning solution used was 1000 ml of hydrochloric acid with 20 g of antimony trioxide and 50 g of stannous chloride. Weight loss ΔW_l was calculated as:

$$\Delta W_l = W_i - W_f \quad (3)$$

where W_i , and W_f are initial and final weights (g) of bars before and after corrosion.

Corrosion rates were determined using eqn. (4)

$$P_r = \frac{1.116 \times 10^7 \times \Delta W_l}{A \times T} \quad (4)$$

where: P_r = corrosion rate (μm/year); ΔW_l = weight loss (g); A = exposed surface area of rebar (cm^2); and T = exposure time (hours).

Corrosion penetration rates were then converted to corrosion current density I_{corr} (μA/cm^2) using the following formula [Alghamdi and Ahmad 2010].

$$I_{corr} = \frac{P_r}{11.7} \quad (5)$$

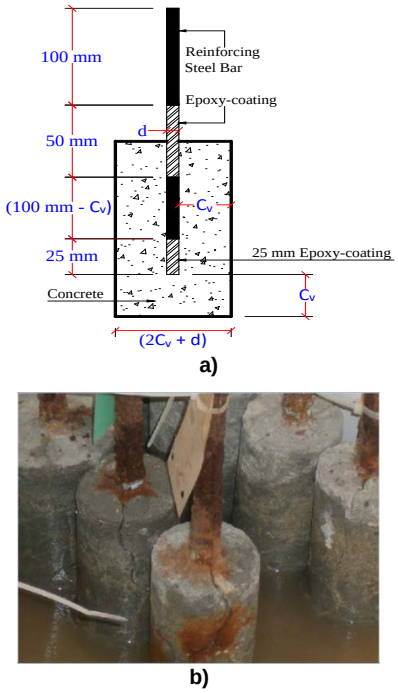

Fig. 1. Test specimens: a) schematic diagram of typical test-specimen; b) typical corrosion state

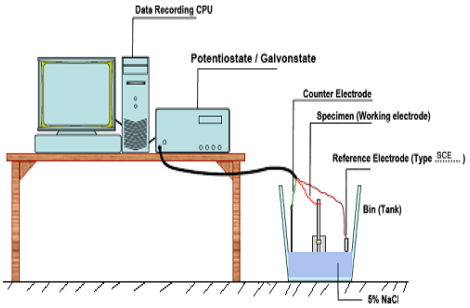

Fig. 2. Schematics of set-up used to determine I_{corr}

3.0 RESULTS AND DISCUSSIONS

3.1 Corrosion-rate patterns with H-type aggregates

The highest and lowest values of corrosion current density measured (Alghamdi and Ahmad 2010) using LPRM for H-type aggregates were noted to be 15.8 μA/cm^2 and 0.39 μA/cm^2, respectively. Generally, it was observed that there is an increase in corrosion current density with an increase in the water/cementitious materials ratio. It was also observed corrosion that the current density decreases with an increase in cover thickness. Another point that was noted is that there is a significant decrease in the rate of corrosion when concrete cover is increased from 25 to 37.5 mm while the decrease in I_{corr} is not that significant when concrete-cover thickness was increased from 37.5 to 50 mm.

Table 2. Compressive strength and modulus of elasticity results of H-type specimens

Mix #	Water-cementitious materials ratio ($R_{w/cm}$)	Cementitious materials content, Q_C (kg/m^3)	Fine/Total aggregate ratio ($R_{FA/TA}$)	28-day compressive strength, f'_c (MPa)	28-day elastic modulus, E_c (GPa)
1	0.38	350	0.35	39.7	36.5
2			0.40	38.8	39.4
3			0.45	39.1	34.7
4		375	0.35	34.1	31.4
5			0.40	38.2	36.5
6			0.45	40.6	38.6
7		400	0.35	34.2	28.6
8			0.40	39.3	38.4
9			0.45	39.8	38.3
10	0.43	350	0.35	27.9	32.7
11			0.40	37.4	37.4
12			0.45	38.5	35.0
13		375	0.35	31.9	31.9
14			0.40	37.1	33.5
15			0.45	33.9	33.9
16		400	0.35	26.5	29.6
17			0.40	30.7	31.3
18			0.45	36.5	30.8
19	0.48	350	0.35	30.0	25.9
20			0.40	32.1	31.5
21			0.45	30.5	31.3
22		375	0.35	20.7	28.0
23			0.40	27.5	27.5
24			0.45	29.9	31.6
25		400	0.35	25.4	26.3
26			0.40	31.0	31.8
27			0.45	25.3	27.7

Table 3: Compressive strength and modulus of elasticity results of T-type specimens

Mix #	Water-cementitious materials ratio ($R_{w/cm}$)	Cementitious materials content, Q_C (kg/m^3)	Fine/Total aggregate ratio ($R_{FA/TA}$)	28-day compressive strength, f'_c (MPa)	28-day elastic modulus, E_c (GPa)
1	0.42	350	0.35	21.6	22.03
2			0.40	25.3	26.2
3			0.45	31	25.78
4		375	0.35	23.3	17.5
5			0.40	27	28.26
6			0.45	30.7	25.36
7		400	0.35	24.6	21.27
8			0.40	27	24.64
9			0.45	28.9	30.93
10	0.47	350	0.35	20.3	23.27
11			0.40	22.8	22.53
12			0.45	25.4	25.4
13		375	0.35	20.8	18.45
14			0.40	26.1	25.95
15			0.45	30.4	30.23
16		400	0.35	22.9	20.94
17			0.40	23.7	22.03
18			0.45	26.5	28.06
19	0.52	350	0.35	19.1	20.86
20			0.40	27.9	26.78
21			0.45	30.9	29.37
22		375	0.35	16.6	17.2
23			0.40	24	21.73
24			0.45	25.8	23.58
25		400	0.35	16	15.56
26			0.40	21.6	19.3
27			0.45	25.2	21.4

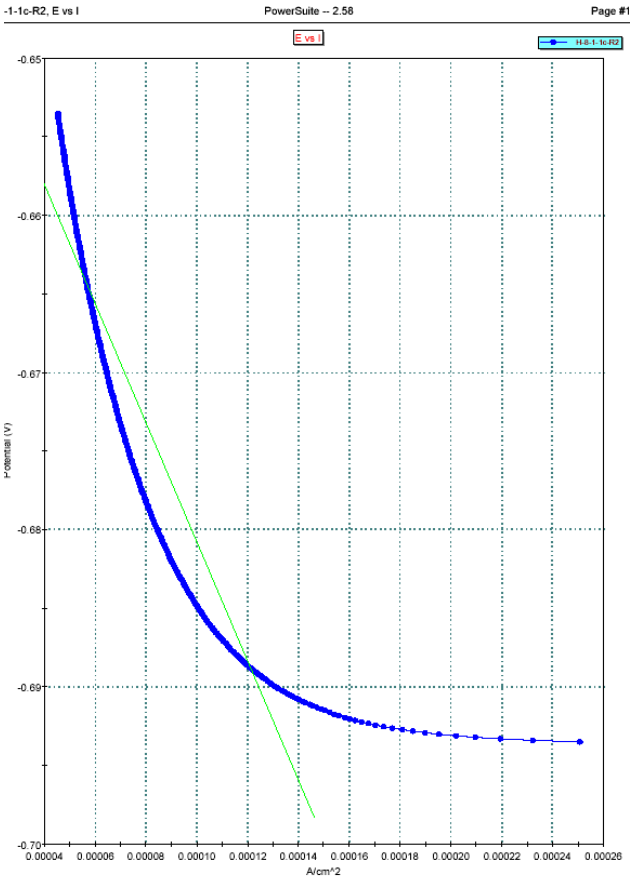

Fig. 3. LPR curve data for specimen AH-8-1-1c in round R-2 [AH-8: w/c=0.40; CC= 400; FA/TA=0.40; f_c'=39.3 MPa; E= 38.4 GPa]

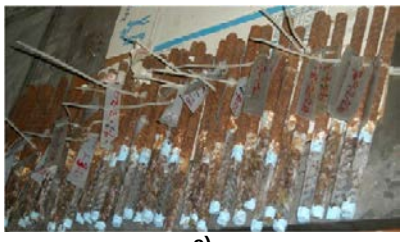

a)

b)

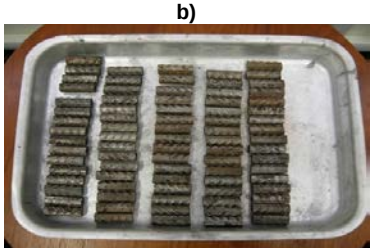

c)

Fig. 4. Typical arrangements of test specimen being prepared for GWLM evaluations

Further, corrosion current density was generally observed to increase as chloride concentration increased from 3 to 12%. It was observed that values of corrosion current density decreases with an increase in cementitious materials content from 350 to 400 kg/m^3. Moreover, it was observed (Alghamdi and Ahmad 2010) there is no clear trend in values of corrosion current density when fine to total aggregate ratio increases, which may be attributed to the fact that increase in fine to total aggregate ratio from 0.35 to 0.45 does not significantly improve the quality of concrete matrix.

The highest and lowest values of corrosion current density $I_{corr,g}$ determined using GWLM were found to be 13.68 µA/cm^2 and 0.48 µA/cm^2, respectively, and the pattern of $I_{corr,g}$ values were found to be similar to $I_{corr,e}$ values determined by of LPR method.

3.2 Corrosion-rate patterns with T-type aggregates

The lowest and highest values of corrosion current density $I_{corr,e}$ determined using LPRM were observed to be 1.06 µA/cm^2 and 17.26 µA/cm^2, *respectively*. Test results indicate that increasing concrete-cover thickness has a noticeable influence, in lowering I_{corr} values. However, while it was observed that there is no significant decrease in the values when cover was increased from 37.5 to 50 mm, the effect on I_{corr} is significant when the cover-value was increased from 25 to 37.5 mm. Moreover, while it was noted that corrosion current density increased with an increase in water-cementitious materials ratio, the effect of fine to total aggregate ratio is minor and no clear influential-trend on I_{corr} values were observed from increasing the fine to total aggregate ratio. This may be attributed to the fact that an increase in fine to total aggregate ratio from 0.35 to 0.45 does not significantly change the quality of concrete matrix.
The lowest and highest values of equivalent corrosion current density determined using GWLM were noted to be 0.52 µA/cm^2 and 14.92 µA/cm^2, respectively, and the patterns of $I_{corr,g}$ values were found to be also similar to the values obtained using the LPR method.

3.3 Variance analysis of corrosion rates data

Statistical Analysis of Variance (**ANOVA**) of test results (shown in Table 4) was carried out using MINITAB software [MINITAB 2000] to assess the effect of independent variables the corrosion current density, I_{corr} values. **ANOVA** is used as a means to evaluate the degree of effect an independent variable (*predictor*) has on dependent variable (*response*). For this purpose, the following notations are used:

$I_{corr,e}$ = Electrochemically measured corrosion current density (µA/cm^2)
$I_{corr,g}$ = Gravimetrically measured corrosion current density (µA/cm^2)
$R_{W/C}$ = Water to cementitious materials ratio by mass
$R_{F/T}$ = Fine to total aggregate ratio by mass
C_C = Cementitious material content (kg/m^3)
C_V = Protective-concrete cover thickness (mm)
C_L = Chloride concentration (% by weight)

Results obtained from **ANOVA** for $I_{corr,e}$ and $I_{corr,g}$ are presented in Tables 4 and 5, respectively. The results presented confirm that, apart from the fine to total aggregate ratio, all the factors have significant effect on corrosion current density

Table 4. ANOVA* for electrochemically measured corrosion rate, $I_{corr,e}$ (Ref. H-type aggregates)

Factor	Type	Levels	Values		
$R_{W/C}$	Fixed	3.00	0.40	0.45	0.50
C_C	Fixed	3.00	350.0	375.0	400.0
$R_{F/T}$	Fixed	3.00	0.35	0.40	0.45
C_L	Fixed	3.00	0.03	0.07	0.12
C_V	Fixed	3.00	25.00	37.50	50.00
Source	**DF**	**SS**	**Adj. MS**	**F**	**P**
$R_{W/C}$	2	882.27	441.13	393.40	0.000
C_C	2	195.69	97.85	87.26	0.000
$R_{F/T}$	2	20.71	10.36	9.24	0.000
C_L	4	54.14	27.07	24.14	0.000
C_V	4	1560.62	780.31	695.87	0.000

Table 5. ANOVA* for gravimetrically measured corrosion rate, $I_{corr,g}$ (Ref. H-type aggregates)

Factors	Type	Levels	Values		
$R_{W/C}$	Fixed	3.00	0.40	0.45	0.50
C_C	Fixed	3.00	350.00	375.00	400.00
$R_{F/T}$	Fixed	3.00	0.35	0.40	0.45
C_L	Fixed	3.00	0.03	0.07	0.12
C_V	Fixed	3.00	25.00	37.50	50.00
Source	**DF**	**SS**	**Adj. MS**	**F**	**P**
$R_{W/C}$	2	527.20	263.60	218.16	0.000
C_C	2	79.20	39.60	32.77	0.000
$R_{F/T}$	2	4.58	2.29	1.90	0.152
C_L	4	25.70	12.85	10.64	0.000
C_V	4	930.69	465.35	385.14	0.000

*Notes:
DF is the number of observations that can be varied independently;
SS is the sum of squared data-points difference from sample mean of *n* data points;
Adj. MS is the measure of variability of group mean around grand mean;
F-*value* is a statistical measure of significance calculated by analysis of variance (**ANOVA).**
P-*ratio* is a statistical measure of acceptance or rejection of a significance that no more than 5% of computed statistical variation is due chance or sampling error.

3.4 Effect of w/c ratio on concrete pore structure

Analysis of concrete matrix (for test specimens prepared from mixture with high and low w/c ratios), using scanning electron microscope (SEM; Stutzman 2000), reveals typical effects of reducing w/c on concrete microstructure that would have ensuing consequences on concrete durability. Typical results obtained from Scanning Electron micrographs of test=specimens having w/c ratio values of 0.4, 0.45

and 0.5 are given in Figures 5, 6, and 7 and in Table 6. These typical results highlight effects of water-cementitious materials ratio on concrete morphology and elemental composition of concrete matrix. Figure 5(a)- shows typical micrograph of concrete specimens prepared with w/c ratio of 0.4. A dense morphology of calcium silicate hydrate (C-S-H) overlaid by calcium hydroxide crystals is noted. The energy dispersive X-ray analysis (EDAX) shows mainly the presence of Si, Ca, Al, Fe and Cl. Similar SEM and EDAX analysis of concrete test-specimens prepared with w/c ratios of 0.45 were done and sample results are given in Table 6 and in Figure 6(a). Analysis of SEM-micrograph of specimens prepared with a w/c ratio of 0.50 (see Figure 7(a)), indicates that structure of C-S-H matrix is porous with predominant presence of ettringite crystals and calcium hydroxide as noted in the pores of the C-S-H matrix. EDAX analysis also shows presence of Mg, Al, Si, Ca, Fe and Cl. A comparison of the SEM-based results also indicates that C-S-H matrix becomes more *porous* with an *increase in the w/c* ratio. Elemental composition (noted from EDAX analysis and summarized in Table 6) further indicates that chloride concentration increases with increase in w/c ratio, with the percentage increase in chloride concentration being about 4.2% when w/c ratio is increased from 0.4 to 0.45, while it is *only* about 0.58% when ratio is increased from 0.45 to 0.50. Analysis of SEM results for three groups of test specimens also emphasizes unfavorable increase in porosity of concrete-matrix.

Table 6. Spectrum of concrete test-specimens with three values of *w/c* ratio

w/c ratio	Spectrum (%)							
	O	**Na**	**Mg**	**Al**	**Si**	**Cl**	**Ca**	**Fe**
0.40	50.6	3.3	1.1	7.2	18.5	2.1	15.8	1.5
0.45	39.3	—	2.0	2.7	15.3	6.3	32.5	2.0
0.50	32.5	—	1.6	6.5	8.5	6.9	39.8	4.2

4.0 CONCLUSIONS

Based on analysis of results obtained in this study, the following conclusions were drawn:

i) Corrosion current density I_{corr} values determined using both LPRM and GWLM for both types of aggregates generally increased with an increase in the water-cementitious materials ratio. Results from this study affirms that service life of RC structure would increase with use of lower values of *w/c* ratio. This is because corrosion current density I_{corr} (used as performance indicator) used for service life prediction of RC structures was found to *decrease* with lower values of w/c ratio.

ii) In all cases considered, the corrosion current density I_{corr} values decrease with an increased in the cover thickness from 25 to 50 mm. As concrete-cover thickness influences corrosion of reinforcing steel, and its quality influences the diffusion rate of oxygen through concrete matrix, the findings of this study are in agreement with the findings of other researchers, that there is a significant increase in the time required for chloride ions to reach steel reinforcing bars with increasing cover thickness, which in turn would extend the service life of RC structures.

iii) Corrosion current density increased with an increase in chloride concentration. This finding confirm other findings (reported in the literature) that corrosion current density I_{corr} values increase with an increase in chloride concentration.

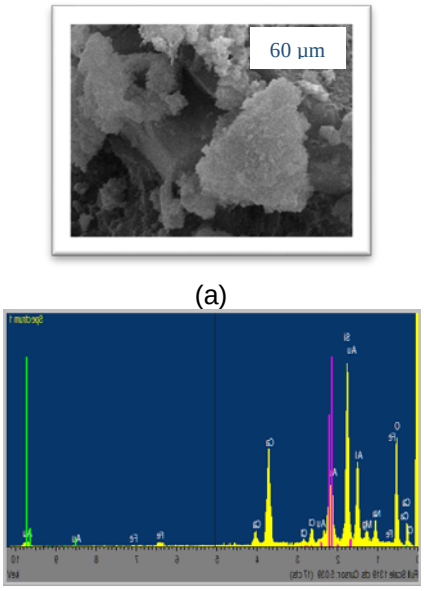

(a)

(b)

Fig. 5. Pore structure and composition-spectrum for concrete test-specimen (*w/c* = 0.40)

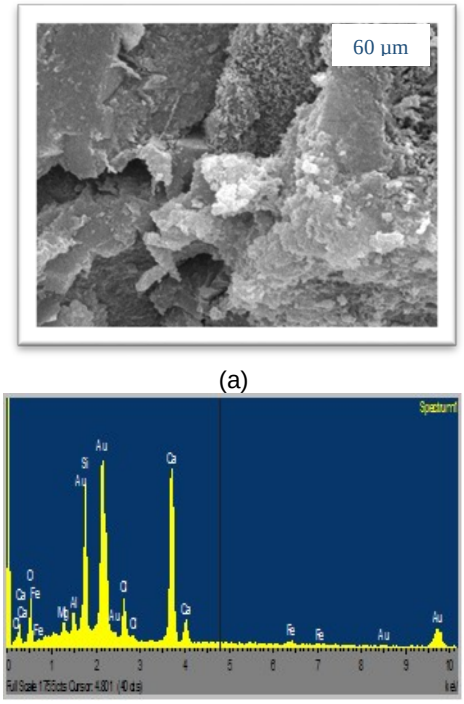

(a)

(b)

Fig. 6. Pore structure and composition-spectrum for concrete test-specimen (*w/c* = 0.45)

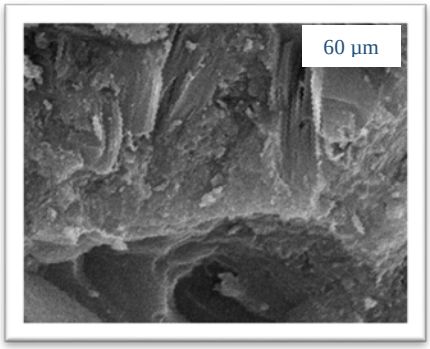

(a)

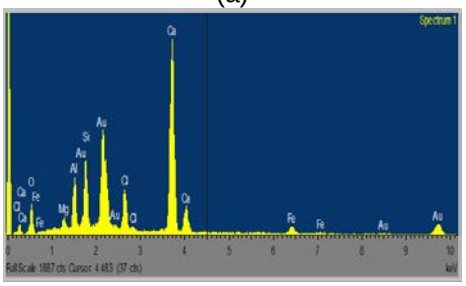

(b)

Fig. 7. Pore structure and composition-spectrum for concrete test-specimen (*w/c* = 0.50)

iv) Results of *variance analysis* indicated that (with exception of results determined by gravimetric weight loss method indicating that fine to total aggregate ratio would not have statistical significance in predicting corrosion current density I_{corr}) all design variables considered in this study had statistically significant influence on corrosion current density.

v) The results obtained have been implemented within an algorithmic design-methodology for durability-based design of RC-structural members (e.g. beams and columns) for targeted service life (specified *a priori*) as a design constraint.

Acknowledgement

This research works was supported by research grant (KACST AT-23-21) provided by KACST, Riyadh, KSA. The financial and logistical supports provided by both KACST and CEE-Department at KFUPM-Dhahran are acknowledged with appreciation.

References

ACI 222R-01, 2001. Protection of Metals in Concrete Against Corrosion. American Concrete Institute, pp. 2-4.

Ahmad, S., Bhattacharjee, B., 1995. A Simple arrangement and procedure for in-situ measurement of corrosion rate of rebar embedded in concrete. Corrosion Science, 37(5): 781-791.

Ali S.I., 2003. Effects of aggregate quality on reinforcement corrosion. MSc Thesis, King Fahd University of Petroleum and Minerals, Dhahran.

Alghamdi, S.A., Ahmad S., 2010. Multi-criteria optimal designs of RC beams and columns – experimental and analytical studies. Final Report, KACST Project AT-23-21.

Al-Tayyib, A.J., Khan, M.S. 1988. Corrosion rate measurement of reinforcing steel in concrete by electrochemical techniques. ACI Materials J., May-June: 172-177.

ASTM C33-03, 2004. Standard specification for concrete aggregate. ASTM International, West Conshohocken.

ASTM C 128-07a, 2003. Standard test method for density, relative density (specific gravity), and absorption of fine aggregate. ASTM, West Conshohocken, Pa.

ASTM G 1-03, 2003. Standard practice for preparing, cleaning, and evaluating corrosion test specimens. West Conshohocken, PA.

Bentur A., Diamond S., Berke N.S., 1997. Steel corrosion in concrete: fundamentals and civil engineering practice. E&FN Spon, London, UK, 201.

Dyer, T., 2014. Concrete durability. CRC Press, Taylor & Francis Group, United Kingdom.

Federal Highway Administration, 2001. Material and method for corrosion control of reinforced and pre-stressed concrete structures in new construction. US Department of Transportation, 630 Georgetown Pike, Mclean VA 22101-2296
Pub. No. 00-081: 1-29.

Ferreira, R.M., 2010. Optimization of RC structure performance in marine environment. Engineering Structures, 32: 1489-1494.

Gehlen, Ch., Schiessl, P. 1999. Probability-based durability design for the western Scheldt Tunnel. Structural Concrete, P1(2): 1-7.

Mehta, P.K., 1977. Effect of cement composition on corrosion of reinforcing steel in concrete. Chloride Corrosion of Steel in Concrete, ASTM STP 629: 12-19.

MINITAB Statistical Package, 2000. Release 13, Minitab Inc.

Morinaga, S., 1990. Prediction of service lives of reinforced concrete buildings based on the corrosion rate of reinforcing steel. Conference Proceedings, Building Materials and Components, Brighton (UK, Nov. 7-9): 5-16.

Oh, B.H., Jang, B.S., Lee, S.C., 2004. Chloride diffusion and corrosion initiation time of reinforced concrete structures. Proceedings, International Workshop on Microstructure and Durability to Predict Service Life of Concrete Structures Sapporo, Japan.

Page, C.L., Short, N.R., Holden, W.R., 1986. The influence of different cements on chloride-induced corrosion of reinforcing steel. Cement and Concrete Research, 16 (1): 79-86.

Page C.L., 1996. Corrosion of reinforcement in concrete construction. The Royal Society of Chemistry, Cambridge, p. 55.

Park, J.I., Bae, S. H., Yu, K.G. Lee, K.M., Choi, S., 2008. Factors influencing the service life of concrete structures exposed to coastal environment. ACF 3rd International Conference-ACF/VCA:1090-1095.

Power-CORR User's Manual, 2001. Corrosion Measurement Software. Princeton Applied Research, USA.

Stern, M., Geary, A.L., 1957. Electrochemical polarization: I. Theoretical analysis of the shape of polarization curves. *Journal of the Electrochemical Society*, 104(1): 56-63.

Stutzman, P.W, 2000. Scanning electron microscopy in concrete petrography. Proceedings, Workshop on the Role of Calcium Hydroxide in Concrete. The American Concrete Society. Nov. 1-3: 59-72.